# Supporting Information

## Mendillo et al. 10.1073/pnas.0912250106

### SI Materials and Methods

**Plasmid and Strain Construction.** MutS-205 (pRDK1395), MutS-211 (pRDK1396), MutS211,2 (pRDK1391), MutS-214,5 (pRDK1392), MutS-675 (pRDK1393), and MutS-679 (pRDK1394) expression plasmids (Table S1) were made by side-directed mutagenesis of pTX412 (pET15b-$His_6$-MutS; a gift of Malcolm Winkler) (1).

The *E. coli* MutS domain II sequence encoding amino acids 116–266 was amplified by PCR with a forward primer containing a NdeI restriction site and a reverse primer containing a BamHI restriction site and was ligated into pET15b-$His_6$MBP (pRDK1232), yielding pRDK1409, which fused domain II of MutS to the C terminus of $His_6$MBP. *S. cerevisiae* Msh2 domain II (amino acids 121–294) and Msh6 domain II (amino acids 420–613) were similarly fused to the C terminus of $His_6$MBP to make pRDK1410 and pRDK1411, respectively.

*msh2–235* (pRDK1397), *msh2–237* (pRDK1398), *msh2–241* (pRDK1399), and *msh2–249* (pRDK1400) were made by site-directed mutagenesis of an *MSH2* low-copy-number *URA3* plasmid (pRDK361). *msh6–541A* (pRDK1401), *msh6–541B* (pRDK1402), *msh6–558A* (pRDK1403), *msh6–558B* (pRDK1404), and *msh6–573* (pRDK1405) were made by site-directed mutagenesis of an *MSH6* low-copy-number *LEU2* plasmid (pRDK439). *msh2–237* (pRDK1406), *msh2–241* (pRDK1408), and *msh2–249* (pRDK1407) were made by site-directed mutagenesis of an *MSH2* plasmid for overexpression in *E. coli* (pLANT–Msh2; gift of Manju Hingorani) (2). *Msh2-msh6–573* (pRDK1520) was made by site-directed mutagenesis of an *MSH2-MSH6* plasmid for dual overexpression in *E. coli* (pET11a-Msh2-Msh6; gift of Manju Hingorani) (2).

The *E. coli* strains used for in vivo analysis were constructed by PCR-mediated recombination in the MG1655 strain TP798 (Δ*(recC-ptr-recB-recD)*::*Ptac-gam-bet-exo-cat*), which conditionally expresses the bacteriophage lambda Red system (3). Briefly, plasmids were engineered with the desired *mutS* allele and its stop codon, with the kanamycin resistance (*kan*$^r$) gene immediately downstream, followed by an additional 50 bases of homology to *mutS* immediately downstream of the stop codon. This construct was used to replace the *bla* gene in RDK4782 (4), which is located after codon 11 of the chromosomal *mutS* locus. This resulted in strains with the *kan*$^r$ gene after the stop codon of the *mutS-205* allele (RDK5012), *mutS-211* allele (RDK5013), and wild-type allele (RDK5011), as well as after codon 11, yielding *mutS*Δ*11* (RDK5014), for use as a null allele (Table S2).

**Protein Expression and Purification.** $His_6$-MutS, $His_6$-MutL, Msh2-Msh6, Mlh1-Pms1, all MBP fusions, and all of the mutant derivatives were expressed and purified as previously described with minor modifications (1, 2, 4–6). pLANT-*MSH2* plasmids and the mutant derivatives were cotransformed with pET11a-*MSH6* into *E. coli* BL21-CodonPlus(DE3)-RIPL (Stratagene) to overexpress wild-type and *msh2* mutant Msh2–Msh6 complexes. The dual-expression plasmids pET11a-*MSH2-MSH6* and pET11a-*MSH2-msh6–573* were similarly transformed to overexpress wild-type and *msh6* mutant Msh2–Msh6 complexes. The LacI protein was provided by Kathleen Matthews (Rice University).

**DXMS.** DXMS analysis was performed as previously described (7–10). MutS, GT mispair containing DNA (71 bp), and ATP with or without MutL in 10 μL of buffer containing 20 mM Tris (pH 8), 4 mM $MgCl_2$, 230 mM NaCl, 4 mM DTT, and 10% glycerol was mixed with 30 μL of $D_2O$ containing 5 mM Tris (pH 8.0), 4 mM $MgCl_2$, 50 mM NaCl, and 250 μM ATP (final concentrations were 3.6 μM MutS, 4.0 μM DNA, 4.0 μM MutL, 250 μM ATP, and 95 mM NaCl) and incubated for 30, 100, 300, 1,000, and 3,000 sec at 4 °C. At the indicated times, the sample was added to vials containing 60 μL of quench solution (0.8% formic acid and 0.8 M GuHCl) and immediately frozen at −80 °C. In addition, a nondeuterated sample (incubated in $H_2O$ buffer) and a fully deuterated sample (incubated in $D_2O$ buffer containing 0.5 M GuHCl for 16 h at 25 °C) were prepared.

The 100-μL samples were manually thawed and immediately passed through an immobilized protease column (66-μL bed volume) of porcine pepsin (Sigma) coupled to 20AL support (PerSeptive Biosystems) at a flow rate of 100 μL/min. Proteolytic fragments were collected contemporaneously on a C18 HPLC column (Vydac) and eluted by a linear gradient (5–45% solvent B in 30 min, 50 mL/min: solvent A, 0.05% TFA; solvent B, 80% acetonitrile, 0.01% TFA). Mass spectrometric analysis was performed using a Thermo Finnigan LCQ mass spectrometer operated with capillary temperature at 200 °C and spray voltage of 5,000 V. Deuterium quantification data were collected in MS1 profile mode, and peptide identification data were collected in MS2 mode. The SEQUEST software program (Thermo Finnigan) was used to identify the likely sequence of the parent peptide ions. Identified peptides were examined to determine whether the quality of the measured isotopic envelope of peptides was sufficient to allow accurate measurement of the geometric centroid of isotopic envelopes on deuterated samples. Specialized software was used to determine deuterium content in functionally deuterated samples as previously described (8, 10).

**SPR Analysis.** Biacore experiments were performed using a Biacore T100 (GE Healthcare) biosensor. A 236-bp DNA substrate that was biotinylated at one end, contained either a central GT mispair or GC base pair, and had the *lac* $O_1$ operator sequence incorporated at the other end, was made as described previously (6) and immobilized to a streptavidin-coated SA Biacore chip.

Experiments analyzing the binding of MutS, Msh2–Msh6, or the mutant complexes on GT mispair or GC base pair substrates were performed essentially as described previously (6). Briefly, 50 nM of MutS or 20 nM Msh2–Msh6 protein was flowed over the DNA substrates in running buffer consisting of 25 mM Tris (pH 8.0), 110 mM NaCl, 4 mM $MgCl_2$, 0.5 mM DTT, 2% glycerol, 0.05%, and IGEPAL CA-630 (Nonidet P-40). After equilibrium was reached, a second injection with running buffer containing 250 μM ATP was flowed over the DNA substrates, and dissociation of the MMR protein complexes was observed.

For experiments examining sliding on end-blocked DNA substrates, 30 nM LacI and 250 μM ATP was included in the running buffer, during both the equilibration and MutS binding phases (6, 11). The baseline of the association curves of MutS depicted was taken after LacI was bound to the DNA substrates, so the binding curves reflect association of MMR proteins only. The sliding of MMR proteins off of the end of the DNA substrate was monitored by performing a second injection that was exactly the same as the first except additionally containing 1 mM IPTG. This allowed dissociation of LacI bound ($T_{1/2}$ ≈1.6 sec) at the ends of the DNA substrate without significantly altering the concentrations of protein in solution. Control experiments were performed that did not contain LacI.

Analysis of MutL binding to the MutS–DNA complex or

Mlh1–Pms1 to the Msh2–Msh6–DNA complex was performed as described, with minor modifications (11). Briefly, 50 nM of MutS with or without 50 nM MutL protein was flowed over the DNA substrates in running buffer. Immediately after, a second injection that was exactly the same as the first was performed, except additionally containing 250 $\mu$M ATP and MutL binding was monitored; MutL does not interact with MutS and DNA in the absence of ATP. Analysis of Msh2–Msh6 with Mlh1–Pms1 included LacI to prevent ternary complex from binding to the ends of the DNA substrates. Briefly, an injection of 30 nM of LacI was first flowed over the indicated DNA substrate. A second injection containing 5 nM Msh2–Msh6 in running buffer containing 250 $\mu$M ATP and 30 nM LacI was performed. Immediately after, a third injection was performed with exactly the same buffer as the previous step, except with or without 25 nM Mlh1–Pms1. All experiments were performed at 25 °C.

**Amylose Pulldowns.** Binding reactions containing 1.5 $\mu$M MBP or the MBP–MutS-DII fusion were incubated in 50 $\mu$L of buffer containing 20 mM Tris (pH 7.5), 4 mM $MgCl_2$, and 70 mM NaCl on ice for 20 min. In addition, the reactions contained 3.5 $\mu$M of MutL and 250 $\mu$M ATP, ATP$\gamma$S, or ADP, as indicated. The incubation was followed by addition of 100 $\mu$L amylose resin (New England Biolabs; resuspended in above buffer) for an additional 15 min. After extensive washes, bound proteins were eluted with 100 $\mu$L buffer containing 20 mM maltose, separated by SDS-PAGE and silver-stained. Experiments analyzing formation of Mlh1–Pms1 with MBP, MBP–Msh2-DII, or MBP–Msh6-DII were performed similarly, except that after separation by SDS-PAGE, Mlh1–Pms1 was detected with an immunoblot using an anti-flag antibody specific for the Flag tag on the C terminus of Pms1.

**Genetic Analysis in *E. coli*.** Rates of accumulating rifampicin resistance mutations were determined by fluctuation analysis using at least 15 independent cultures for each strain (12–14). Cultures were grown overnight, and dilutions were plated on LB plus 50 $\mu$g/ml kanamycin with or without 100 $\mu$g/mL rifampicin and incubated overnight at 37 °C. Two-tailed Mann-Whitney tests were performed to calculate *P* values using Graphpad Prism version 4.0b for Macintosh (Graphpad Software).

**Genetic Analysis in *S. cerevisiae*.** The *S. cerevisiae* strains used were isogenic derivatives of the S288c strain RDKY3686 (*MAT*$\alpha$ *ura3–52 leu2*$\Delta$*1 trp1*$\Delta$*63 his3*$\Delta$*200 hom3–10 lys2–10A*) (15). RDKY3688 has an *msh2*::*hisG* mutation and RDKY4234 has *msh3*::*hisG* and *msh6*::*hisG* mutations. Plasmids containing mutant *MSH2* or *MSH6* alleles were transformed into strain RDKY3688 (*msh2*$\Delta$) and RDKY4234 (*msh3*$\Delta$ *msh6*$\Delta$), respectively, and were analyzed as described previously (16). Briefly, transformants were patched onto media lacking Ura for the *MSH2* plasmids or lacking Leu for the *MSH6* plasmids to maintain plasmid selection. Patches were then replica plated onto plates lacking Ura or Leu and Lys or Ura or Leu and Thr and grown at 30 °C for 2 to 3 days to select for *lys2–10A* and *hom3–10* revertants to visualize mutator phenotypes.


1. Feng G, Winkler ME (1995) Single-step purifications of His6-MutH, His6-MutL and His6-MutS repair proteins of *Escherichia coli* K-12. *Biotechniques* 19:956–965.
2. Antony E, Hingorani MM (2003) Mismatch recognition-coupled stabilization of Msh2-Msh6 in an ATP-bound state at the initiation of DNA repair. *Biochemistry* 42:7682–7693.
3. Poteete AR, Fenton AC, Nadkarni A (2004) Chromosomal duplications and cointegrates generated by the bacteriophage lamdba Red system in *Escherichia coli* K-12. *BMC Mol Biol* 5:22.
4. Mendillo ML, Putnam CD, Kolodner RD (2007) *Escherichia coli* MutS tetramerization domain structure reveals that stable dimers but not tetramers are essential for DNA mismatch repair in vivo. *J Biol Chem* 282:16345–16354.
5. Mazur DJ, Mendillo ML, Kolodner RD (2006) Inhibition of Msh6 ATPase activity by mispaired DNA induces a Msh2(ATP)-Msh6(ATP) state capable of hydrolysis-independent movement along DNA. *Mol Cell* 22:39–49.
6. Mendillo ML, Mazur DJ, Kolodner RD (2005) Analysis of the interaction between the *Saccharomyces cerevisiae* MSH2-MSH6 and MLH1-PMS1 complexes with DNA using a reversible DNA end-blocking system. *J Biol Chem* 280:22245–22257.
7. Black BE, Brock MA, Bedard S, Woods VL, Jr, Cleveland DW (2007) An epigenetic mark generated by the incorporation of CENP-A into centromeric nucleosomes. *Proc Natl Acad Sci USA* 104:5008–5013.
8. Brock M, et al. (2007) Conformational analysis of Epac activation using amide hydrogen/deuterium exchange mass spectrometry. *J Biol Chem* 282:32256–32263.
9. Melnyk RA, et al. (2006) Structural determinants for the binding of anthrax lethal factor to oligomeric protective antigen. *J Biol Chem* 281:1630–1635.
10. Pantazatos D, et al. (2004) Rapid refinement of crystallographic protein construct definition employing enhanced hydrogen/deuterium exchange MS. *Proc Natl Acad Sci USA* 101:751–756.
11. Hess MT, Mendillo ML, Mazur DJ, Kolodner RD (2006) Biochemical basis for dominant mutations in the *Saccharomyces cerevisiae* MSH6 gene. *Proc Natl Acad Sci USA* 103:558–563.
12. Lea DE, Coulson CA (1948) The distribution of the numbers of mutants in bacterial populations. *J Genet* 49:264–285.
13. Luria SF, Delbruck M (1943) Mutations of bacteria from virus sensitivity to virus resistance. *Genetics* 28:491–511.
14. Miller J (1992) *A Short Course in Bacterial Genetics* (Cold Spring Harbor Lab Press, Cold Spring Harbor, NY).
15. Amin NS, Nguyen MN, Oh S, Kolodner RD (2001) exo1-Dependent mutator mutations: Model system for studying functional interactions in mismatch repair. *Mol Cell Biol* 21:5142–5155.
16. Shell SS, Putnam CD, Kolodner RD (2007) Chimeric *Saccharomyces cerevisiae* Msh6 protein with an Msh3 mispair-binding domain combines properties of both proteins. *Proc Natl Acad Sci USA* 104:10956–10961.

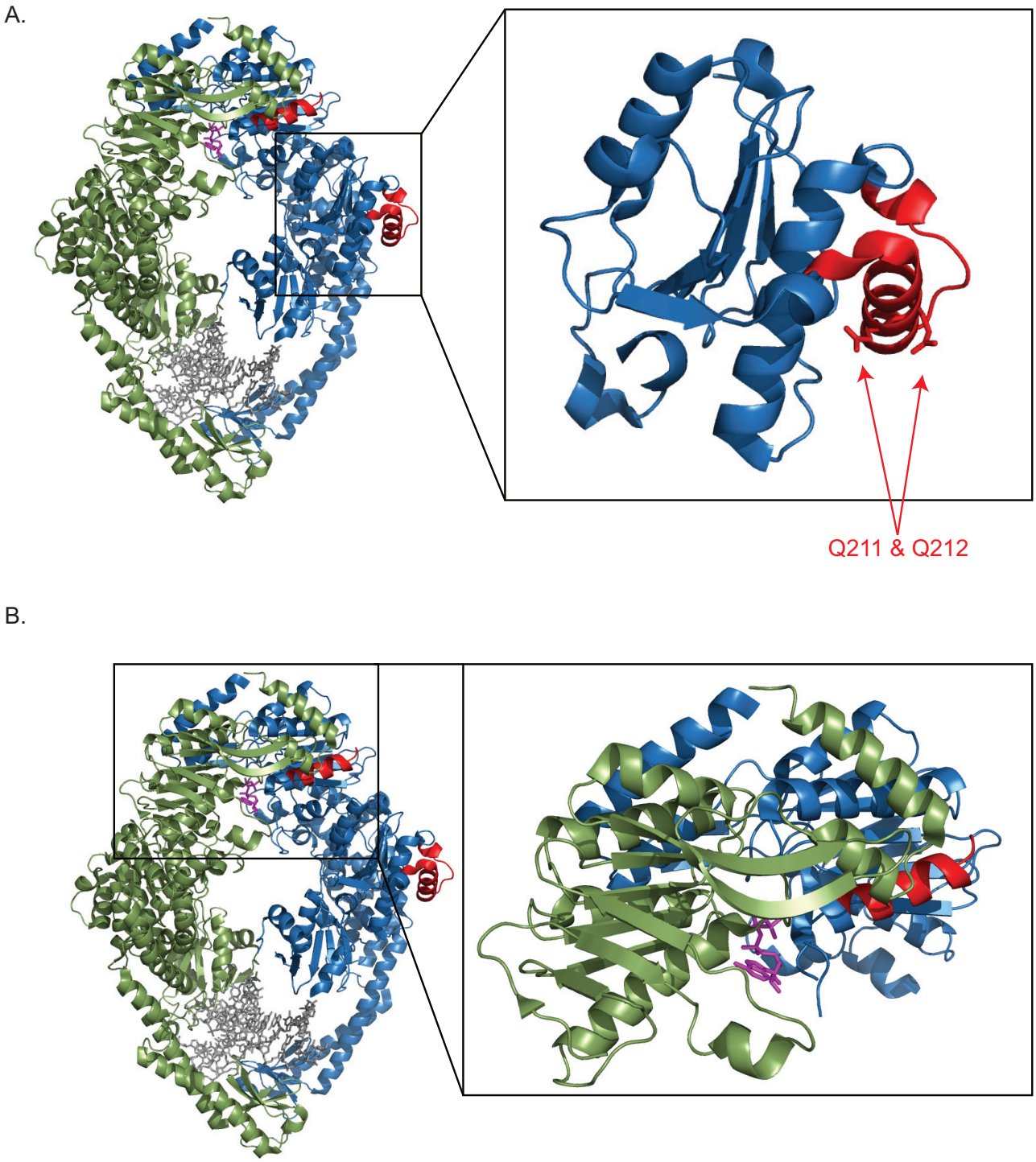


**Fig. S1.** Two regions of MutS with MutL-dependent reduced deuteration. Region A from 204–225 and region B from 673–686 are shown in red on the non-mispair contacting subunit of MutS (PDB ID code 1w7a) [Lamers MH, et al. (2004) ATP increases the affinity between MutS ATPase domains. Implications for ATP hydrolysis and conformational changes. *J Biol Chem* 279:43879–43885]. (*A*) Region A is shown in the context of domain II. (*B*) Region B is shown in the context of the ATPase domains with the ATP of the other MutS subunit of the homodimer highlighted in magenta.

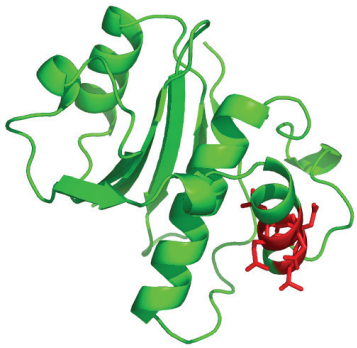

**mutS-211**
QQLNL-211-215-
SSLSS

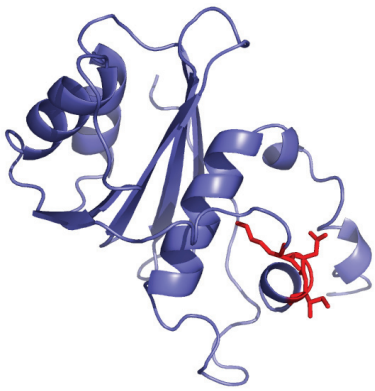

**msh2-235**
KDV-235-237-DDS
(hMsh2: KDI)

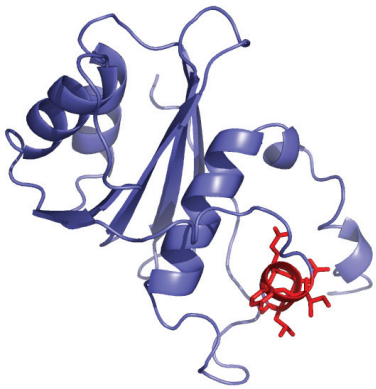

**msh2-237**
VELDL-237-241-
SSLSS
(hMsh2: IYQDL)

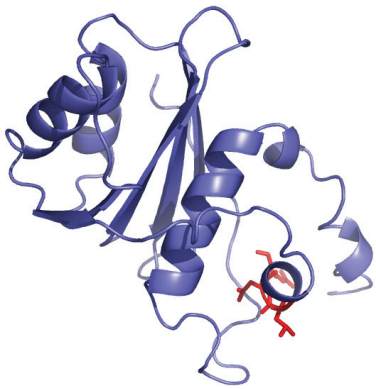

**msh2-241**
LTK-241-243-STD
(hMsh2: LNR)

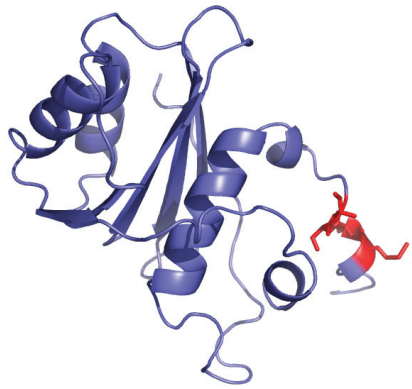

**msh2-249**
LAL-249-251-SAS
(hMsh2: MNS)

**Fig. S2.** Structural conservation of Msh2 domain II with MutS domain II in the region altered in MutS-211. Residues mutated in *S. cerevisiae* Msh2 in the same region as the *E. coli mutS-211* mutations (PDB ID code 1w7a, green) are colored red on the model of *H. sapiens* Msh2 domain II (PDB ID code 2o8b, violet).

**Table S1. Plasmids**

| Plasmid name | Allele | Amino acid substitutions | Strain no. |
|---|---|---|---|
| pTX412 (pET15b-His6-MutS) | *mutS* | — | (1) |
| pRDK1391 (pET15b-His6-MutS-211,2) | *mutS-211,2* | Q211S Q212S | RDK5054 |
| pRDK1392 (pET15b-His6-MutS-214,5) | *mutS-214,5* | N214S L215S | RDK5055 |
| pRDK1393 (pET15b-His6-MutS-675) | *mutS-675* | T675K E676K | RDK5057 |
| pRDK1394 (pET15b-His6-MutS-679) | *mutS-679* | N679S H682S N683S | RDK5058 |
| pRDK1395 (pET15b-His6-MutS-205) | *mutS-205* | E205S D207S | RDK5059 |
| pRDK1396 (pET15b-His6-MutS-211) | *mutS-211* | Q211S Q212S N214S L215S | RDK5060 |
| pRDK361 (pRS316-*MSH2*) | *MSH2* | — | RDK3512 |
| pRDK1397 (pRS316-*msh2–235*) | *msh2–235* | K235D V237S | RDK5033 |
| pRDK1398 (pRS316-*msh2–237*) | *msh2–237* | V237S E238S D240S L241S | RDK5034 |
| pRDK1399 (pRS316-*msh2–241*) | *msh2–241* | L241S K243D | RDK5035 |
| pRDK1400 (pRS316-*msh2–249*) | *msh2–249* | L249S L251S | RDK5036 |
| pRDK439 (pRS315-*MSH6*) | *MSH6* | — | RDK3572 |
| pRDK1401 (pRS315-*msh6–541A*) | *msh6–541A* | D541K D543K | RDK5044 |
| pRDK1402 (pRS315-*msh6–541B*) | *msh6–541B* | D541S D543D K544K | RDK5045 |
| pRDK1403 (pRS315-*msh6–558A*) | *msh6–558A* | E558K E559K D560K | RDK5046 |
| pRDK1404 (pRS315-*msh6–558B*) | *msh6–558B* | E558S E559S D560S | RDK5047 |
| pRDK1405 (pRS315-*msh6–573*) | *msh6–573* | K573D K574D | RDK5048 |
| pLANT-*MSH2* | *MSH2* | — | (2) |
| pRDK1406 (pLANT-Msh2–237) | *msh2–237* | V237S E238S D240S L241S | RDK5049 |
| pRDK1408 (pLANT-Msh2–241) | *msh2–241* | L241S K243D | RDK5051 |
| pRDK1407 (pLANT-Msh2–249) | *msh2–249* | L249S L251S | RDK5050 |
| pET11a-*MSH6* | *MSH6* | — | (2) |
| pET11a-*MSH2-MSH6* | *MSH2, MSH6* | — | (2) |
| pRDK1520 (pET11a-Msh6–573) | *MSH2, Msh6–573* | K573D K574D | RDK5245 |
| pRDK1232 (pET15b-His6-MBP) | MBP | — | RDK5031 |
| pRDK1409 (pET15b-His6-MBP-MutSDII) | MBP-MutS domain II | — | RDK5062 |
| pRDK1410 (pET15b-His6-MBP-Msh2DII) | MBP-Msh2 domain II | — | RDK5066 |
| pRDK1411 (pET15b-His6-MBP-Msh6DII) | MBP-Msh6 Domain II | — | RDK5067 |


1. Feng G, Winkler ME (1995) Single-step purifications of His6-MutH, His6-MutL and His6-MutS repair proteins of *Escherichia coli* K-12. *Biotechniques* 19:956–965.
2. Antony E, Hingorani MM (2003) Mismatch recognition-coupled stabilization of Msh2-Msh6 in an ATP-bound state at the initiation of DNA repair. *Biochemistry* 42:7682–7693.

**Table S2. Bacterial strains**

| Strain no. | Genotype | Mutation/amino acid substitution |
|---|---|---|
| TP798 | Δ *(recC-ptr-recB-recD)*::*Ptac-gam-bet-exo-cat mutS*::*kan* | — |
| RDK4782 | TP798 *mutSΔ11*::*bla* | Deletion after codon 11 |
| RDK5011 | TP798 *mutS*::*kan* | — |
| RDK5012 | TP798 *mutS-205*::*kan* | E205S D207S |
| RDK5013 | TP798 *mutS-211*::*kan* | Q211S Q212S N214S L215S |
| RDK5014 | TP798 *mutSΔ11*::*kan* | Deletion after codon 11 |